ChemComm

Accepted Manuscript

This article can be cited before page numbers have been issued, to do this please use: M. E. Witzke, P. Dietrich, M. Y. S. Ibrahim, K. Al-Bardan, M. D. Triezenberg and D. Flaherty, *Chem. Commun.*, 2016, DOI: 10.1039/C6CC08305F.

ROYAL SOCIETY OF CHEMISTRY

rsc.li/chemcomm

ROYAL SOCIETY OF CHEMISTRY View Article Online
DOI: 10.1039/C6CC08305F

Journal Name

COMMUNICATION

Spectroscopic Evidence for Origins of Size and Support Effects on Selectivity of Cu Nanoparticle Dehydrogenation Catalysts

Received 00th January 20xx,
Accepted 00th January 20xx

DOI: 10.1039/x0xx00000x

www.rsc.org/

M. E. Witzke,[§a] P. J. Dietrich,[§b] M. Y. S. Ibrahim,[a] K. Al-Bardan,[a] M. D. Triezenberg,[a] and D. W. Flaherty*[a]

Selective dehydrogenation catalysts that produce acetaldehyde from bio-derived ethanol can increase the efficiency of subsequent processes such as C-C coupling over metal oxides to produce 1-butanol or 1,3-butadiene or oxidation to acetic acid. Here, we use *in situ* X-ray absorption spectroscopy and steady state kinetic experiments to identify $Cu^{\delta+}$ at the perimeter of supported Cu clusters as the active site for esterification and Cu^0 surface sites as sites for dehydrogenation. Correlation of dehydrogenation and esterification selectivities to *in situ* measures of Cu oxidation states show that this relationship holds for Cu clusters over a wide-range of diameters (2-35 nm) and catalyst supports and reveals that dehydrogenation selectivities may be controlled by manipulating either.

Biomass has been targeted as a potentially renewable source of carbon for the production of fuels and chemicals due to concerns regarding sustainability and global climate change.[1,2] In particular, ethanol (C_2H_5OH) is an appealing building block for longer chain oxygenates and hydrocarbons because of recent improvements in the efficiency of fermentation processes.[3,4] C_2H_5OH-derived C_2 units can be used to produce a number of commodity chemicals (e.g., 1-butanol and higher alcohols,[5] C_8 aromatics,[6] and ethyl acetate[7]) using an array of condensation reactions.[8] Most of these reactions proceed via coupling reactions involving carbonyl groups of aldehydes or ketones, which requires highly selective (>95%) dehydrogenation of C_2H_5OH and other alcohols to avoid yield losses.[4,5] Copper (Cu) catalysts give high selectivities for alcohol dehydrogenation, in part, because Cu (as well as Ag[9] and Au) cleaves C-C and C-O bonds at much lower rates than other transition metals (e.g., Pd, Pt, Ni).[10,11] Esterification is the major side reaction over both heterogeneous[12-17] and homogeneous Cu catalysts,[18,19] and this undesirable pathway decreases dehydrogenation yields and reduces the value of the products stream for fuel and lubricant applications.[9] Despite the importance of dehydrogenation and esterification reactions as intentional and unintentional reactions catalyzed by supported Cu clusters, the chemical nature and the location of the active site for each category of reactions remains unclear despite previous reports regarding the effects of Cu cluster size,[13,15,20] support,[12,21,22] oxidation state,[14,20] and preparation methods.[12,21,23]

Here, we use a combination of *in situ* X-ray absorption spectroscopy, steady-state rate measurements, and reaction inhibition studies to demonstrate that dehydrogenation occurs on Cu^0 sites and esterification proceeds on $Cu^{\delta+}$ sites that exist only at the perimeter of the interface between Cu clusters and the support. The relative populations of exposed Cu^0 and $Cu^{\delta+}$ sites depend sensitively on the cluster size and the support identity.

Figure 1 shows that the selectivity for dehydrogenation (i.e., formation of acetaldehyde, C_2H_4O) is 10^1-10^3 times greater than that for esterification, and 10^2-10^4 times greater than that for all other reactions and depends on ethanol conversion (X_{EtOH}) on 6 nm Cu clusters formed upon the surface of CrO_x by the reduction of commercial 2CuO Cr_2O_3 in

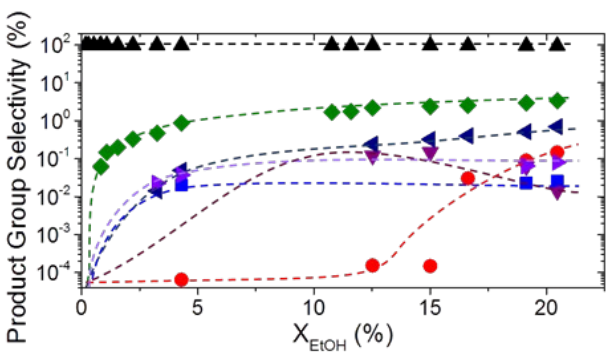

Fig. 1 Changes in selectivity for dehydrogenation (▲), esterification (◆), ketonization (◀), decarbonylation (●), aldol addition (▶), etherification (▼), and dehydration (■) as functions of X_{EtOH} on 6 nm Cu-CrO_x (2.75 kPa C_2H_5OH, 15 kPa H_2, 503 K). Lines are intended to guide the eye.

[a] *Department of Chemical and Biomolecular Engineering, University of Illinois Urbana-Champaign, Urbana, IL 61801. Email: dwflhrty@illinois.edu*
[b] *BP Group Research, Naperville, IL 60563*
§ These authors contributed equally.
† Electronic Supplementary Information (ESI) available: Catalyst synthesis and characterization procedures; TEM and cluster size distributions; LCs for TPR-XANES; XRD patterns; selectivity and rate measurements. See DOI: 10.1039/x0xx00000x

H_2, hereafter referred to as Cu-CrO_x (2.75 kPa C_2H_5OH, 15 kPa H_2, 83.6 kPa He, 503 K). Esters account for the largest amount of carbon lost at these conditions and on other Cu catalysts (e.g., Cu-SiO_2, Cu-ZnO, and Cu-TiO_2, Table S1). Esterification rates and selectivities are immeasurable at low X_{EtOH} (Fig. 1), which shows that esters do not form by primary reaction between two C_2H_5OH molecules, but rather form by a secondary reaction that involves a reactive intermediate derived from C_2H_5OH, consistent with previous studies.[12,24,25] Moreover, esterification rates are >20 times smaller in the absence of C_2H_5OH in comparison with those measured in mixtures of C_2H_5OH, H_2, and C_2H_4O reactants (Table S2). Esters form on homogeneous (CuBr,[18,19] and $Cu(OAc)_2$[19]) and heterogeneous catalysts (Cu,[22,26,27] Cu-SiO_2,[13,16,22] Cu-Cr_2O_3,[12,27] and Cu-Zn-Zr-Al-O[25]) by the coupling of an alcohol and an aldehyde,[19,25] whereas basic metal oxides (e.g., MgO and CaO)[28] form esters via the Tishchenko reaction between two aldehydes.[28-30] Taken together, the observations that ethyl acetate ($C_4H_8O_2$) forms by secondary reactions of C_2H_5OH (Figure 1) and that esterification rates are insignificant in pure C_2H_4O streams (Table S2) suggest that C_2H_4O reacts with a C_2H_5OH derived intermediate to form $C_4H_8O_2$ as suggested previously.[13,25] Here, rate inhibition and X-ray absorption spectra are combined to identify the chemical nature and likely location of the active sites responsible for the formation of $C_4H_8O_2$.

The active sites for esterification on supported Cu cluster catalysts have been associated with the Cu dispersion,[13] prevalent oxidation state of the Cu,[12,14,17] and Lewis acidic sites of the metal oxide support[31] in a series of independent studies. Colley *et al*. concluded that active sites for the formation of $C_4H_8O_2$ are located on Cu rather than the Cr_2O_3 support of commercial Cu-Cr_2O_3,[27] while Moromi *et al*. suggested that C_2H_5OH and C_2H_4O couple on Pt-SnO_2 at Lewis acid sites presented by the support (Sn^{4+}).[31] Others have suggested Cu^+ as the active site for esterification,[14,20,32] which is consistent with recent comparisons of the number of Cu-ZrO_2 interfacial sites to $C_4H_8O_2$ formation rates on CuZr-SiO_2 catalysts.[17] However, these hypotheses have not been proven to hold for series of Cu clusters supported on multiple reducible and irreducible supports, or to correlate with Cu^+ populations; therefore, the origin and control of the active site(s) remains unknown. Figure S1 shows that pyridine (0.1-2.5 kPa) inhibits esterification rates on 6 nm Cu-CrO_x catalysts at 503 K. Esterification rates that decrease with increasing pyridine pressure, combined with evidence from Colley *et al.*[27] identifying Cu as the active site on Cu-Cr_2O_3, strongly suggests that Lewis acid sites (e.g., Cu^+, Cu^{2+}) bind active intermediates that form $C_4H_8O_2$. Thus, it seems likely that Lewis acidic Cu sites remain even after *in situ* reductive treatments or reform upon the introduction of C_2H_5O and C_2H_4O.

In contrast with previous studies that correlate esterification rates to the number of $Cu^{\delta+}$ species measured *ex situ* using XPS[14] or adsorbed CO in FTIR,[17] *in situ* X-ray absorption near edge structure (XANES) spectra provide a direct measurement of the distribution of Cu oxidation states (i.e., Cu^0, Cu^+, and Cu^{2+}) present following reductive treatments and at conditions used for C_2H_5OH dehydrogenation. Figure S2 shows that XANES spectra of supported Cu catalysts (on SiO_2, C, TiO_2, ZnO, and unsupported Cu) measured following *in situ* reduction (40 kPa H_2, 60 kPa He, 573 K) do not change after introduction of the reactant mixture for 30 min (4 kPa C_2H_5OH, 0.75 kPa C_2H_4O, 0.25 $C_4H_8O_2$, 30 kPa H_2, bal. He, 503 K) within the uncertainty of the technique. These data strongly suggest that oxidation states measured at a given temperature during temperature programmed reduction-XANES (TPR-XANES) experiments match those present during C_2H_5OH dehydrogenation experiments measured under strict kinetic control.

Ester formation rates normalized by total Cu atoms measured at X_{EtOH} = 10% (Fig. S5, 503 K, 2.75 kPa C_2H_5OH, 15 kPa H_2, 83.6 kPa He) decrease with increasing particle diameter as $r_{ester} \sim d^{-1.3 \pm 0.2}$ for SiO_2 supported Cu catalysts, which suggests that esterification may occur on under coordinated sites such as edges, corners, or perimeter sites at the interface of the Cu clusters and the support.[33] While r_{ester} depends monotonically on the diameter of Cu clusters on Cu-SiO_2, esterification selectivities vary by an order of magnitude for a given Cu cluster diameter across multiple catalyst supports (e.g., SiO_2, C, TiO_2, CrO_x, Al_2O_3, etc.) and do not correlate with Cu cluster size when the identity of the support also changes (Fig. S6). Taken together, the number of esterification sites, depends on both the support identity and the cluster size. This suggests that active sites for ester formation exist at the perimeter of the cluster-support interface and not on metal terraces,[13] which are minimally influenced by the support. These perimeter sites may be Lewis acidic $Cu^{\delta+}$ species, as implied by pyridine inhibition measurements (Fig. S1). The importance of $Cu^{\delta+}$ for esterification reactions can be directly tested by correlating XANES measurements with selectivity measurements, as described below.

Figure 2a shows XANES spectra obtained at the Cu-K edge

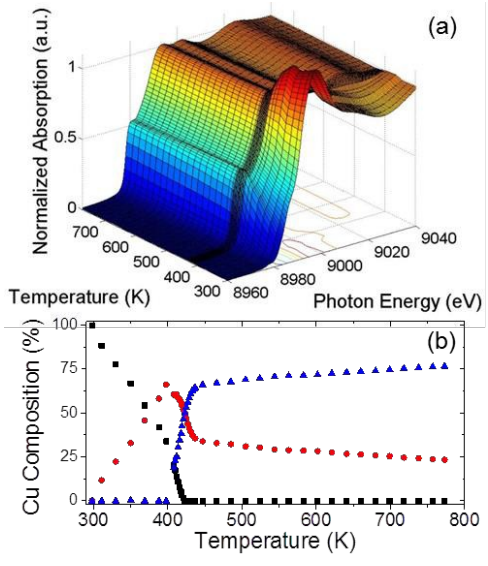

Fig. 2 a) TPR-XANES spectra of Cu-K edge on 2 nm Cu-SiO_2, and b) change in the distribution of Cu in Cu^{2+} (■), Cu^+ (●), and Cu^0 (▲) oxidation states during *in situ* reduction from 298 K – 773 K, 5 K min^{-1} in 40% H_2/60% He.

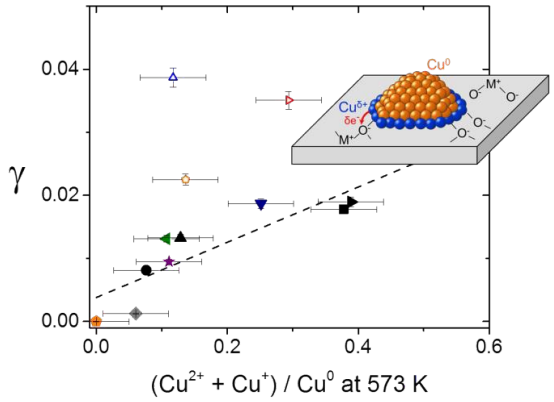

Fig. 3 γ ($r_{ester}/r_{dehydro}$) correlate with the ratio of $Cu^{\delta+}$ to Cu^0 species at 573 K for Cu catalysts including Cu supported on ZnO-Al_xO_y (▼), TiO_2 (△), Al_xO_y (▷), SiO_2 (2 nm, ▶; 3 nm, ■; 8 nm, ▲; 35 nm, ●), C (8 nm, ★), ZnO (◆) CrO_x (◀), Raney Cu(⬠), and unsupported Cu (⬟). Insert illustrates $Cu^{\delta+}$ atoms at the cluster perimeter. Rates are measured at X_{EtOH} = 10% (2.75 kPa C_2H_5OH, 15 kPa H_2, 83.6 kPa He, 503 K) and corrected for the approach to equilibrium. Linear fit (dashed) includes all filled symbols.

(8980 eV) during TPR of 2 nm Cu-SiO_2 (40 kPa H_2, 303-773 K, 5 K min^{-1}), and the changes in the spectral line shape with increasing temperature reflect the stepwise reduction of Cu atoms (Cu^{2+}→Cu^+→Cu^0). Figure 2b shows the mole fraction of Cu in each oxidation state as a function of temperature (oxidation state distributions at 573 K for all other Cu catalysts are provided in SI, Table S7). The fractions of Cu^{2+}, Cu^+, and Cu^0 present during C_2H_5OH dehydrogenation were calculated from TPR-XANES curves at the reaction temperature, assuming that oxidation states do not change with the introduction of oxygenates (Figs. S2 and S3).

Figure 3 shows the correlation between the ratio of rates for $C_4H_8O_2$ and C_2H_4O formation (γ, where $\gamma = r_{ester}/r_{dehdro}$) and the ratio of ($Cu^{2+}$ + Cu^+) to Cu^0 present in Cu nanoparticles supported on two classes of materials, which are described individually. For all materials, the measured ratio of (Cu^{2+} + Cu^+) to Cu^0 gives a quantitative measure of the reducibility of Cu and encompasses all indirect factors that affect the extent of charge transfer from Cu atoms to the support or adsorbates. Charge transfer at the interface between the metal cluster and the support forms exposed $Cu^{\delta+}$ sites around the cluster perimeter, as described for Cu-CeO_2,[34] Pt-SiO_2,[35] and Au-TiO_2.[36] The bulk ratio of (Cu^{2+} + Cu^+) to Cu^0 measured by XANES also represents that of exposed Cu species available for catalysis, if we assume that $Cu^{\delta+}$ species can exist only at the cluster-support interface and that the Cu clusters are hemispherical (derivation in ESI, Equation S1).

First, values of γ linearly correlate to the ratio of (Cu^{2+} + Cu^+) to Cu^0 for catalysts that do not contain a second metal oxide component that can independently facilitate esterification (i.e., SiO_2, C, ZnO, ZnO-Al_xO_y, Cr_2O_3, and unsupported Cu powder; filled symbols, Fig. 3). Among these materials, values of γ do not depend solely on the diameter of Cu clusters, or the identity of the support, rather γ is a complex function of both. This correlation (Fig. 3) provides compelling evidence that exposed $Cu^{\delta+}$ species (and not Cu^0), present at the interface between Cu clusters and supports, are the predominant active sites for esterification on inert catalyst supports.

Second, Cu clusters in contact with metal oxides that independently catalyze esterification (i.e., TiO_2, co-precipitated Cu-Al_xO_y, and Raney Cu; hollow symbols, Fig. 3) lie above the linear trend line, because TiO_2,[37-39] and Al_xO_y[39-41] catalyze ester formation even in the absence of Cu. In addition, Raney Cu produced from CuAl alloys contains trace Al, as demonstrated by compositional analysis (Table S4), that may form Al_xO_y *in situ*. Al_xO_y and TiO_2 catalysts prepared without Cu show significant selectivities for esterification (Table S3); however, rates associated with the support cannot be directly subtracted from the total esterification rates on Cu-Al_xO_y and Cu-TiO_2 because of significant differences between the surface areas and properties of materials made with and without Cu (Table S3). Yet, these data (Fig. 3 and Table S3) show that these Lewis acidic supports catalyze esterification, which increases γ without increased $Cu^{\delta+}$ sites, and are consistent with the hypothesis that Lewis acid sites, whether $Cu^{\delta+}$ or support sites, catalyze esterification.

Scheme 1 shows interdependent catalytic cycles for the esterification of C_2H_5OH that are consistent with $C_4H_8O_2$ formation rates (measured here and previously reported for Cu catalysts)[13,25,26,41] as well as the role of Cu^{2+} and Cu^+ sites in this reaction. Adsorption of C_2H_5OH and C_2H_4O onto unoccupied Cu^0 surface sites to form adsorbed ethanol (C_2H_5OH*) and acetaldehyde (C_2H_4O*) (1.1 and reverse 1.5, respectively), the dissociative adsorption of H_2 (reverse 1.4 and reverse 1.9), and O-H bond rupture to form ethoxide (C_2H_5O*) (1.3) are all assumed to be quasi-equilibrated steps based on previous studies of Cu clusters[13,27,42] and Cu (110)[43] and Cu(111) surfaces.[44,45] The elimination of hydrogen from the carbonyl carbon of C_2H_5O* (1.3) completes dehydrogenation and forms C_2H_4O by subsequent desorption of C_2H_4O* (1.5). The esterification cycle begins with adsorption of C_2H_4O to Cu^{2+} sites (1.6) forming an activated aldehyde intermediate

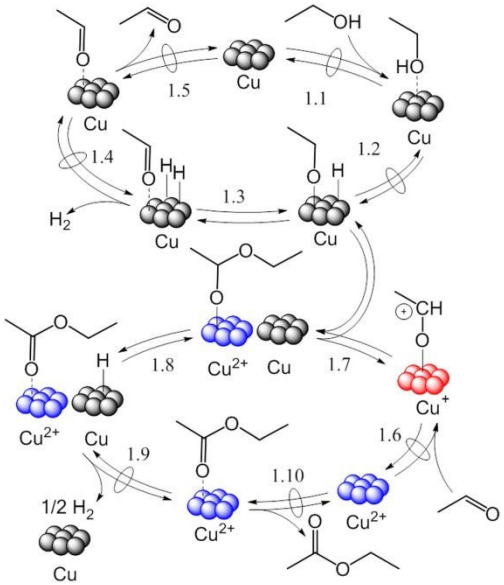

Scheme 1 Proposed mechanism for ethyl acetate formation from ethanol through a dehydrogenation (1.1-1.5) and redox esterification cycle (1.6-1.10) on Cu^0 and $Cu^{\delta+}$.

($C_2H_4O^+$*) on Cu^+. Nucleophilic attack of C_2H_5O* to the carbonyl of $C_2H_4O^+$* reforms Cu^{2+} and a hemiacetal intermediate (1.7), which dehydrogenates to produce $C_4H_8O_2$* and H* (1.8), which desorb (1.9, 1.10). Scheme 1 shows that Lewis acidic Cu^+ sites that bind activated aldehydes interconvert with Cu^{2+} sites within the redox cycle that forms $C_4H_8O_2$, as described for esterification on homogenous Cu catalysts (e.g., $CuBr$[18,19] and $Cu(OAc)_2$).[19]

Overall, the strong correlation between γ and the ratio of the Cu oxidation states, together with the inhibiting effects of pyridine on ester formation rates, provide compelling evidence that $Cu^{\delta+}$ sites participate primarily in the catalytic cycle that produces $C_4H_8O_2$ from reactions of C_2H_4O and C_2H_5OH (Scheme 1) while Cu^0 mainly catalyzes the intervening steps for dehydrogenation. The number of esterification active sites (i.e., $Cu^{\delta+}$ species) depends on the cluster size (i.e., number of perimeter Cu atoms), and the identity of the support, which affects the extent of charge transfer. This work offers insight into possible combinations of characterization methods to identify specific reaction centers and highlights the need to understand and control selectivity of potential reactions of biomass fermentation products to commodity chemicals.

We thank Pranjali Priyadarshini, Daniel T. Bregante, and Rogan Kipp for assistance with experiments. TEM and XRD measurements were carried out in part in the Frederick Seitz Materials Research Laboratory Central Research Facilities, University of Illinois. MRCAT operations are supported by the Department of Energy and the MRCAT member institutions. This research used resources of the Advanced Photon Source, a U.S. Department of Energy (DOE) Office of Science User Facility operated for the DOE Office of Science by Argonne National Laboratory under Contract No. DE-AC02-06CH11357. This work was funded by the Energy Biosciences Institute at the University of Illinois. This material is based upon work supported by the National Science Foundation Graduate Research Fellowship Program under Grant No. DGE - 1144245.

Notes and references

1. R. D. Perlack and B. J. Stokes, *U.S. Billion-Ton Update*, 2011.
2. Y. N. Zeng, S. Zhao, S. H. Yang and S. Y. Ding, *Curr. Opin. Biotechnol.*, 2014, **27**, 38.
3. J. T. Kozlowski and R. J. Davis, *ACS Catal.*, 2013, **3**, 1588.
4. P. Anbarasan, Z. C. Baer, S. Sreekumar, E. Gross, J. B. Binder, H. W. Blanch, D. S. Clark and F. D. Toste, *Nature*, 2012, **491**, 235.
5. T. Moteki and D. W. Flaherty, *ACS Catal.*, 2016, **6**, 4170.
6. T. Moteki, A. T. Rowley and D. W. Flaherty, *ACS Catal.*, 2016, **6**, 7278.
7. M. Eckert, G. Fleischmann, R. Jira, H. M. Bolt and K. Golka, in *Ullmann's Encyclopedia of Industrial Chemistry*, Wiley-VCH Verlag GmbH & Co. KGaA, 2000.
8. L. Wu, T. Moteki, A. A. Gokhale, D. W. Flaherty and F. D. Toste, *Chem*, 2016, **1**, 32.
9. V. L. Sushkevich, I. I. Ivanova and E. Taarning, *ChemCatChem*, 2013, **5**, 2367.
10. M. Y. S. Ibrahim, MS thesis, University of Illinois at Urbana-Champaign, 2015.
11. S. Sitthisa and D. E. Resasco, *Catal. Lett.*, 2011, **141**, 784.
12. E. Santacesaria, G. Carotenuto, R. Tesser and M. Di Serio, *Chem. Eng. J.*, 2012, **179**, 209.
13. M. E. Sad, M. Neurock and E. Iglesia, *J. Am. Chem. Soc.*, 2011, **133**, 20384.
14. Y. Wang, Y. L. Shen, Y. J. Zhao, J. Lv, S. P. Wang and X. B. Ma, *ACS Catal.*, 2015, **5**, 6200.
15. J. C. Kenvin, M. G. White and M. B. Mitchell, *Langmuir*, 1991, **7**, 1198.
16. A. K. Agarwal, M. S. Wainwright, D. L. Trimm and N. W. Cant, *J. Mol. Catal.*, 1988, **45**, 247.
17. I. Ro, Y. Liu, M. R. Ball, D. H. K. Jackson, J. P. Chada, C. Sener, T. F. Kuech, R. J. Madon, G. W. Huber and J. A. Dumesic, *ACS Catal.*, 2016, **10**, 7040.
18. W. J. Yoo and C. J. Li, *Tetrahedron Lett.*, 2007, **48**, 1033.
19. Y. Zheng, W. B. Song and L. J. Xuan, *Org. Biomol. Chem.*, 2015, **13**, 10834.
20. I. C. Freitas, S. Damyanova, D. C. Oliveira, C. M. P. Marques and J. M. C. Bueno, *J. Mol. Catal. A: Chem.*, 2014, **381**, 26.
21. E. Geravand, Z. Shariatinia, F. Yaripour and S. Sahebdelfar, *Chem. Eng. Res. Des.* 2015, **96**, 63.
22. N. Iwasa and N. Takezawa, *Bull. Chem. Soc. Jpn.*, 1991, **64**, 2619.
23. G. Carotenuto, R. Tesser, M. Di Serio and E. Santacesaria, *Catal. Today*, 2013, **203**, 202.
24. X. Y. Liu, B. J. Xu, J. Haubrich, R. J. Madix and C. M. Friend, *J. Am. Chem. Soc.*, 2009, **131**, 5757.
25. K. Inui, T. Kurabayashi and S. Sato, *J. Catal.*, 2002, **212**, 207.
26. K. Takeshita, S. Nakamura and K. Kawamoto, *Bull. Chem. Soc. Jpn.*, 1978, **51**, 2622.
27. S. W. Colley, J. Tabatabaei, K. C. Waugh and M. A. Wood, *J. Catal.*, 2005, **236**, 21.
28. T. Seki and H. Hattori, *Catal. Surv. Asia*, 2003, **7**, 145.
29. L. Kürti and B. Czakó, *Strategic applications of named reactions in organic synthesis : background and detailed mechanisms*, Elsevier Academic, Burlington, MA, 2005.
30. T. Seki, H. Kabashima, K. Akutsu, H. Tachikawa and H. Hattori, *J. Catal.*, 2001, **204**, 393.
31. S. K. Moromi, S. M. A. H. Siddiki, M. A. Ali, K. Kon and K. Shimizu, *Catal. Sci. Technol.*, 2014, **4**, 3631.
32. E. K. Poels and D. S. Brands, *Appl. Catal., A*, 2000, **191**, 83.
33. M. Shekhar, J. Wang, W. S. Lee, W. D. Williams, S. M. Kim, E. A. Stach, J. T. Miller, W. N. Delgass and F. H. Ribeiro, *J. Am. Chem. Soc.*, 2012, **134**, 4700.
34. T. E. James, S. L. Hemmingson and C. T. Campbell, *ACS Catal.*, 2015, **5**, 5673.
35. C. S. Ewing, G. Veser, J. J. McCarthy, J. K. Johnson and D. S. Lambrecht, *J. Phys. Chem. C*, 2015, **119**, 19934.
36. J. Saavedra, H. A. Doan, C. J. Pursell, L. C. Grabow and B. D. Chandler, *Science*, 2014, **345**, 1599.
37. S. Wang, K. Goulas and E. Iglesia, *J. Catal.*, 2016, **340**, 302.
38. J. Fang, F. C. Shi, J. Bu, J. J. Ding, S. T. Xu, J. Bao, Y. S. Ma, Z. Q. Jiang, W. P. Zhang, C. Gao and W. X. Huang, *J. Phys. Chem. C*, 2010, **114**, 7940.
39. K. T. Li and C. K. Wang, *Appl. Catal., A*, 2012, **433**, 275.
40. L. Jun-Cheng, X. Lan, X. Feng, W. Zhan-Wen and W. Fei, *Appl. Surf. Sci.*, 2006, **253**, 766.
41. J. Prasad and P. G. Menon, *J. Catal.*, 1972, **26**, 477.
42. P. Claus, M. Lucas, B. Lucke, T. Berndt and P. Birke, *Appl. Catal., A*, 1991, **79**, 1.
43. C. Ammon, A. Bayer, G. Held, B. Richter, T. Schmidt and H. P. Steinruck, *Surf. Sci.*, 2002, **507**, 845.
44. M. Bowker and R. J. Madix, *Appl. Surf. Sci.*, 1981, **8**, 299.
45. M. Bowker and R. J. Madix, *Surf. Sci.*, 1982, **116**, 549.

